

# Mechanisms for transient localization in a diatomic nonlinear chain

Stefano Lepri<sup>a,b</sup>, Francesco Piazza<sup>c</sup>

<sup>a</sup>*Consiglio Nazionale delle Ricerche, Istituto dei Sistemi Complessi, Via Madonna del Piano 10  
I-50019 Sesto Fiorentino, Italy*

<sup>b</sup>*Istituto Nazionale di Fisica Nucleare, Sezione di Firenze, via G. Sansone 1 I-50019, Sesto  
Fiorentino, Italy*

<sup>c</sup>*Centre de Biophysique Moléculaire, (CBM), CNRS-UPR 4301, Rue C. Sadron, 45071, Orléans,  
France and Université d'Orléans, Château de la Source, 45071 Orléans Cedex, France*

---

## Abstract

We investigate transient nonlinear localization, namely the self-excitation of energy bursts in an atomic lattice at finite temperature. As a basic model we consider the diatomic Lennard-Jones chain. Numerical simulations suggest that the effect originates from two different mechanisms. One is the thermal excitation of genuine discrete breathers with frequency in the phonon gap. The second is an effect of nonlinear coupling of fast, lighter particles with slow vibrations of the heavier ones. The quadratic term of the force generate an effective potential that can lead to transient grow of local energy on time scales the can be relatively long for small mass ratios. This heuristics is supported by a multiple-scale approximation based on the natural time-scale separation. For illustration, we consider a simplified single-particle model that allows for some insight of the localization dynamics.

*Keywords:* Discrete breathers, Nonlinear localization, Diatomic chain

---

## 1. Introduction

Energy transfer among nonlinear systems occurs in many physical context, ranging from condensed matter to optics. For instance, understanding the principles of vibrational energy transport at the nanoscale is a necessary step for thermal management in phononic systems and requires a deeper understanding of the properties of strongly anharmonic and/or disordered crystals and artificial materials. Nonlinear effects are essential in many respects: in the first place, they determine thermal transport properties. This is particularly dramatic in low-dimensions where nonlinear interaction of energy fluctuations lead to anomalous conductivity [1]. Also, nonlinear excitations have proven to be responsible of slow-relaxation phenomena, whose dynamics recalls that of glassy systems despite the fact that disorder is not present (see e.g. [2, 3, 4, 5, 6] and references therein). There is also evidence that self-excitation of DB plays a role in nonequilibrium steady states [7].

The concept of localization due to nonlinearity is well established. For discrete nonlinear systems, the notion of discrete breathers (DB), termed also intrinsic localized modes (ILM) in solid state physics or discrete solitons (DS) in nonlinear optics, is well known.

*Preprint submitted to Elsevier*

*June 8, 2021*

DB are exact time-periodic and spatially localized vibrational modes found generically in nonlinear lattice models, typically independent of the size and dimensionality of the lattice, and of the specific choice of anharmonic potentials. Their existence emerges as a joint effect of anharmonicity (i.e. an energy-dependent frequency of vibration) and discreteness (i.e. the existence of band gaps in the plane-wave spectrum) [8].

A relevant problem is the self-excitation of such localized modes in thermodynamic conditions. This has been studied in the literature for several models [9, 10, 11, 12]. For anharmonic lattices at thermal equilibrium (i.e. at finite energy density) one may expect that DBs may be created as a kind of randomly activated process. Relatively large thermal fluctuations may lead to shift of the local oscillation frequency, that may enter the plane-wave spectral gap. Once formed, such localized modes may stay off-resonance from the linear spectrum allowing the energy to remain confined at a few sites for relatively long times. This manifest as a form of *transient localization*. However, it is not trivial to identify unambiguously the signature of DB directly from equilibrium simulations, i.e. by direct inspection of particle trajectory. Some specific diagnostics has been indeed proposed both in the frequency and time domains [13, 14, 12, 15].

In this work we will address this problem both numerically than analytically for a simple diatomic chain. We argue that transient localization observed empirically originates from two different mechanisms. One is the thermal excitation of genuine DB with frequency in the phonon gap. The second is an effect of nonlinear coupling of fast, lighter particles with slow vibration due to the heavy ones. We illustrate our findings by considering a simple model consisting of particles constrained on the line and interacting with a nearest-neighbor Lennard-Jones potential with diatomic arrangement of masses. The uniform (equal-masses) case has been considered in several papers starting from ref. [16]. A relevant result is that the dynamical correlations function display breakdown of conventional hydrodynamics. This anomaly is traced back by the presence of correlations due to the reduced dimensionality [17]. The existence of DB is proved for alternating mass chains with anharmonic coupling for large enough mass ratio was first proved in [18] and later studied in several works, see e.g [19, 20, 21, 22, 23]. Besides this, diatomic chains have been studied in the non-equilibrium setup for the alternating mass harmonic [24] and anharmonic [25] cases. The chain with alternating bonds has also been considered [26].

The outline of the paper is as follows. In Section 2 we present the model and recall its harmonic approximation in Section 3. Numerical results based on power spectra and wavelet transforms are presented in Section 4. In Section 5 we present an analysis of the case where the mass ratio is small and nonlinearity weak. A novel type of multiple scale expansion is presented yielding approximate equations for the motion of light particles. A simplified single-particle dynamics is illustrated to explain heuristically the transient energy localization mechanism. Finally, a brief summary is given in the last Section.

## 2. The diatomic Lennard-Jones chain

We consider an array of  $N$  point-like atoms ordered along a line. The position of the  $n$ -th atom is denoted with  $x_n$  and let  $m_n$  denote its mass. Assuming that interactions are restricted to nearest-neighbor pairs, the equations of motion write

$$m_n \ddot{x}_n = V'(x_{n+1} - x_n) - V'(x_n - x_{n-1}), \quad (1)$$

where  $V'(z)$  is a shorthand notation for the first derivative of the the interparticle potential  $V$  with respect to  $z$ . The particles are confined in a simulation “box” of length  $L$  with periodic boundary conditions

$$x_{n+N} = x_n + L \quad . \quad (2)$$

Accordingly, the particle density  $d = N/L$  is a state variable to be considered together with the specific energy (energy per particle) that will be denoted by  $e$ . We focus on the Lennard–Jones potential that in our units reads [17]

$$V(z) = \frac{1}{12} \left( \frac{1}{z^{12}} - \frac{2}{z^6} + 1 \right) \quad . \quad (3)$$

For computational purposes, the coupling parameters have been fixed in such a way as to yield the simplest form for the force. With this choice,  $V$  has a minimum in  $z = 1$  and the resulting dissociation energy is  $V_0 = 1/12$ . Notice that for convenience we set the zero of the potential energy in  $z = 1$ . The presence of the repulsive term in one dimension ensures that the ordering is preserved (the particles do not cross each other).

We consider a diatomic chain with  $m_n$  assuming two alternating values  $m$  and  $M$ . Before proceeding, we recall that Huang and Hu [27] argued that the potential (3) satisfies the condition for the existence of optical gap breathers (that they call optical lower cut-off gap soliton modes) if the cubic term in the Taylor expansion is large enough but does not admit acoustic gap breathers nor optical above the optical band. However, acoustic and optical upper cutoff vibrating kinks are possible excitations for these diatomic lattice systems. According to their paper this is true independently of the mass ratio. This property of the diatomic Lennard-Jones potential should be contrasted with other cases like with hard nonlinearity where DB close to the acoustic band can form, see e.g. [26]. In [28] the possibility of more exotic kink-solitons solutions is also demonstrated.

### 3. Harmonic approximation

From now on, we choose to work at a density value  $d = 1$  such that the equilibrium positions of the particles coincide with the minimum of the potential  $V$ . It is convenient to separate the equations of motion for even-numbered (light) and odd-numbered (heavy) particles introducing the displacements  $u_n, v_n$  from equilibrium positions (that in our dimensionless units can be set to  $nl$  with  $l = 1$ ) as  $x_{2n+1} = 2n + 1 + u_n$  (slow) and  $x_{2n} = 2n + v_n$  (fast) [29]. They satisfy the equations ( $F \equiv -V'$ ,  $F(0) = 0$ )

$$\begin{aligned} m\ddot{v}_n &= -F(u_n - v_n) + F(v_n - u_{n-1}) \quad ; \\ M\ddot{u}_n &= -F(v_{n+1} - u_n) + F(u_n - v_n) \end{aligned} \quad (4)$$

For later reference it is useful to recall the harmonic approximation of the chain where  $F(z) \approx -kz$  with  $k = 6$  in our units for  $V$  as given by eq. (3). The phonon bands  $\omega(q)$  for the infinite chain are

$$\omega^2(q) = k \left( \frac{1}{M} + \frac{1}{m} \pm \sqrt{\left( \frac{1}{m} + \frac{1}{M} \right)^2 - \frac{4}{mM} \sin^2(q)} \right) \quad (5)$$

and  $|q| < \pi/2$  is the Brillouin zone. There is a band gap in the linear spectrum defined by the band edges of the acoustic and optical branches:

$$0 < \omega < \sqrt{\frac{2k}{M}}, \quad \sqrt{\frac{2k}{m}} < \omega < \sqrt{2k\left(\frac{1}{m} + \frac{1}{M}\right)}. \quad (6)$$

The sound velocity defined in the small  $q$  limit of the acoustic branch is another relevant scale of the model and is given by

$$v_s = \sqrt{\frac{2k}{m+M}} \quad (7)$$

#### 4. Transient localization

In this section we first illustrate the results of numerical data demonstrating transient localization in the harmonic gap defined by equations (6). We have performed equilibrium microcanonical simulations by integrating Eqs. (1) (with periodic boundary conditions (2) ) by means of a fourth-order symplectic algorithm [30]. Initial positions were chosen to be in the ground state as given in the previous Section. The initial velocities were drawn at random from a Gaussian distribution and rescaled by suitable factors to assign the kinetic energy to the desired value and to set the total initial momentum equal to zero. A suitable transient is elapsed before acquisition of statistical averages. Conservation of energy and momentum was monitored during each run. This check is particularly crucial at high energies/densities where the strongly repulsive part of the force comes into play and may lead to significant inaccuracies. The chosen time-step (0.01) ensures energy conservation up to a few parts per million in the worst case.

In Fig. 1 we show the space-time plots of the local energy

$$e_n = \frac{1}{2}m_n\dot{x}_n^2 + \frac{1}{2}[V(x_{n+1} - x_n) + V(x_n - x_{n-1})]$$

of one representative run. There is a spontaneous localization of energy around well-defined sites where an energy above the average it is seen for a given time. In the rightmost panels the time evolution of local energy and the associated power spectra of the momentum are illustrated. The characteristic oscillation frequency lies in the gap of the linear spectrum just below the optical band, thus supporting the idea that it correspond to excitation of DB with a given lifetime. This concept has been discussed often in the literature for various nonlinear models. From the figure it is nonetheless evident that also other types of localized spots appear throughout the lattice.

A convenient way to analyze non-stationary signals is to use a wavelet analysis in the time-frequency domain. This technique proved to be useful to pinpoint transient vibrational excitations in many-body system starting from simple chain models [13] to simulated NaI crystals [31]. This method allows to detect transient frequency components appearing at specific times and lasting for finite lapses of time. In this work, we have computed the Gabor transform of the momentum of  $n$ th oscillator, namely

$$G_n(\omega, t) = \int_{-\infty}^{+\infty} e^{-(t-\tau)^2/a} e^{-i\omega\tau} p_n(\tau) d\tau \quad (8)$$

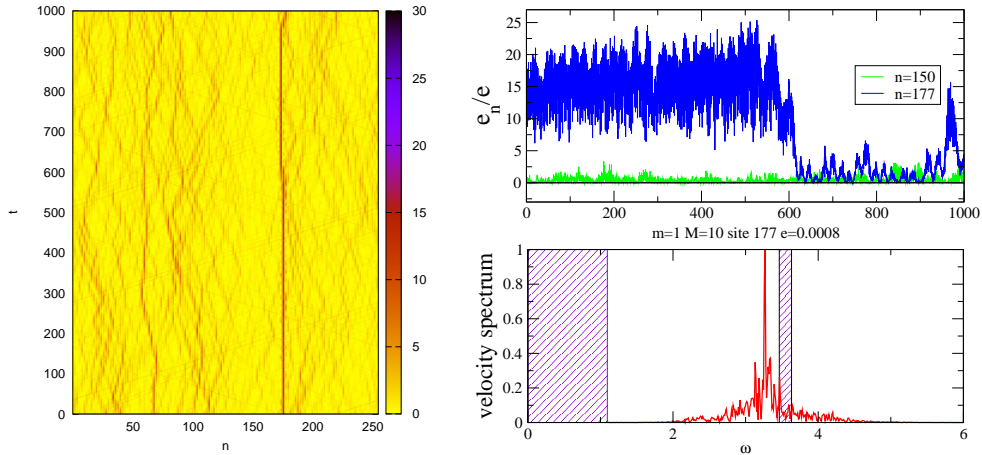


Figure 1: Transient localization of energy in the diatomic Lennard-Jones chain  $N = 256$ ,  $d = 1$ ,  $m = 1$ ,  $M = 10$ . Left: space-time plots of the local energies  $e_n$ . Right upper panel: comparison of time evolutions of energies on the breather site with the one without. Right-lower panel: Fourier spectrum of the momentum of the particle  $n = 177$ , showing the emergence of nonlinear oscillations in the harmonic gap (the shaded area represent the two linear bands given by eq.(6).

In Fig.2 we show  $|G_n(\omega, t)|^2$  for three adjacent sites for the same run as in Fig.1. First of all there is a clear confirmation of the DB oscillations below the optical band. Notice that the signal is present simultaneously on all the three sites in agreement with the idea that the DB is a collective oscillation that involve all the particles, independent of their mass. Besides that there are signatures of transient localization close or below the lower acoustic band edge. This type of events seems to occur independently on neighboring sites.

Besides considering individual trajectories one may look at statistical indicators like correlation functions. We computed the dynamical structure factor, namely the square modulus of temporal Fourier transform of the particle density

$$\rho(q, t) = \frac{1}{N} \sum_n \exp(-iqx_n) \quad , \quad (9)$$

which is defined as

$$S(q, \omega) = \langle |\rho(q, \omega)|^2 \rangle \quad . \quad (10)$$

The square brackets denote an average over a set of independent molecular-dynamics runs. By virtue of the periodic boundaries, the allowed values of the wavenumber  $q$  are integer multiples of  $2\pi/L$ . Data windowing (Hanning window) has been used to compute the FFT in time. We also computed the spectrum of the momenta  $p_n = m_n \dot{x}_n$  of the individual particles

$$s_n(\omega) = \langle |p_n(\omega)|^2 \rangle \quad (11)$$

averaging over independent trajectories. This quantity is related to the incoherent part of the spectrum according to the terminology used in neutron scattering experiments.

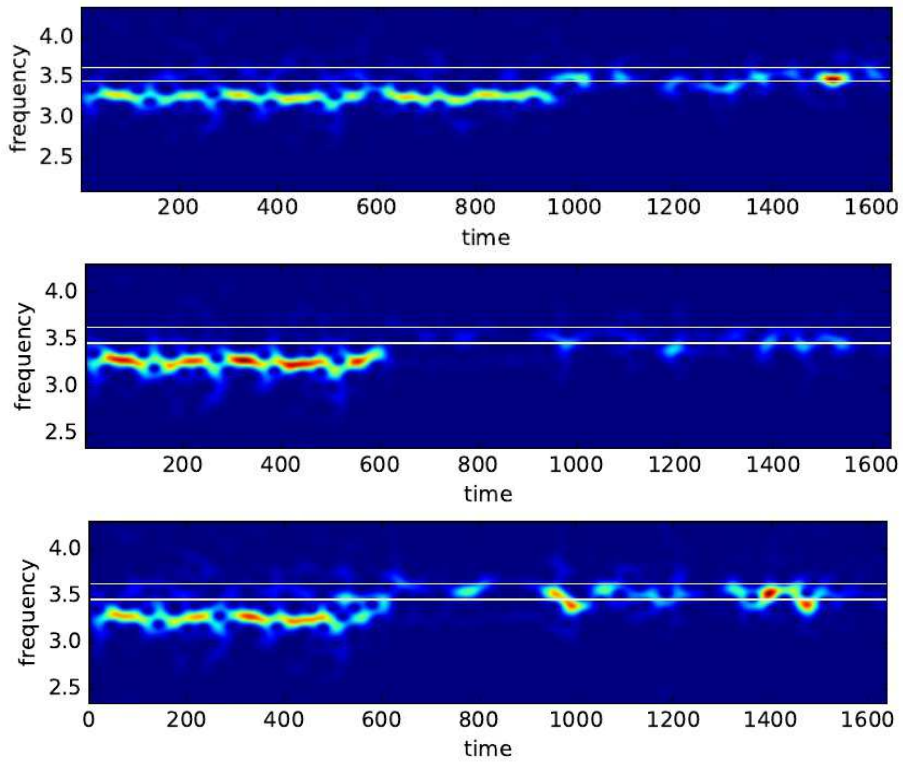


Figure 2: The square modulus of the Gabor transform of momentum for light and heavy particles is different,  $N = 256$ ,  $d = 1$ ,  $m = 1$ ,  $M = 10$ ,  $a = 500$  for three adjacent sites  $n = 176, 177, 178$  (top to bottom). The horizontal lines correspond to the edges of the optical band. Even sites have lighter mass  $m$  and display shorter transient localization slightly below the lower optical band-edge. The signature of the oscillations at a breather frequency 3.3 is seen in all of the neighboring particles.

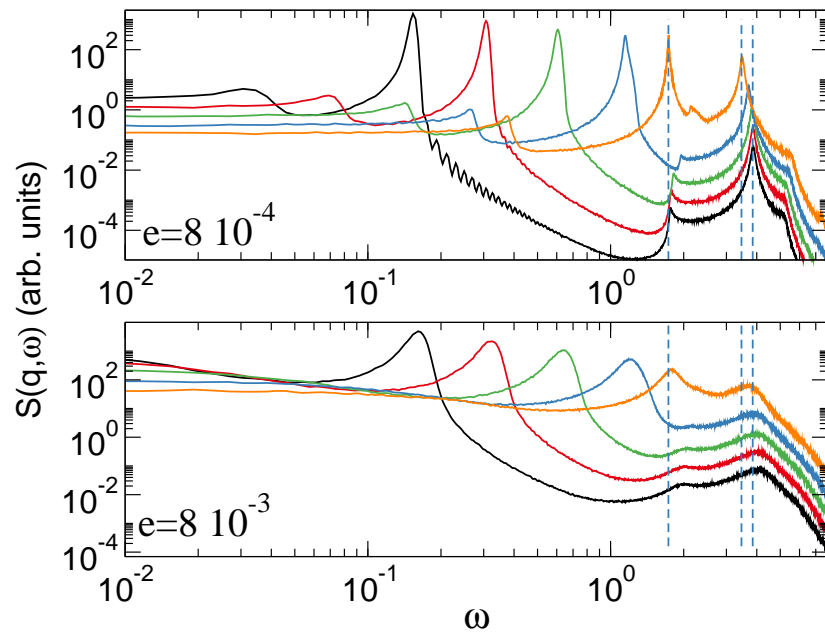


Figure 3: Structure functions for  $q = 0.0981, 0.1963, 0.3926, 0.7853$  and  $\pi/2$  from left to right;  $N = 1024$ ,  $d = 1$ ,  $M = 4$ ,  $m = 1$  the vertical dotted lines are the phonon band edges. Two values of the energy density  $e$  are shown. For larger  $e$  the spectral components in the gap is larger.

In Fig. 3 we plot the structure factors for two different values of the energy density  $e$  and different wavenumbers  $q$ . The main peaks are in good agreement with the phonon frequencies calculated from eq. (5). What appears is that, upon increasing the energy density there is an increasingly larger spectral component within the band-gap, that signals the enhancement of gap oscillations due to nonlinearity. Moreover, the largest frequency component in the gap occurs for wavenumbers closer to the zone boundary,  $q \approx \pi/2$  meaning that the nonlinear effects and transient localization is, as expected, associated to short-wavelengths dynamics.

In Fig.4 we compare the spectra  $s_n$  of light and heavy particles, as given by definition (11), for two different mass ratios. To improve statistics an averaging over a subset of about 10 particles with the same mass is performed. As expected from the harmonic approximation, it is seen that light particles oscillate faster with frequencies around the optical band and a weak spectral component in the acoustic band. Such a component reduces upon increasing the mass ratio. Moreover, there is an increasing sizeable component in the gap that can be attributed to the localized excitations described above.

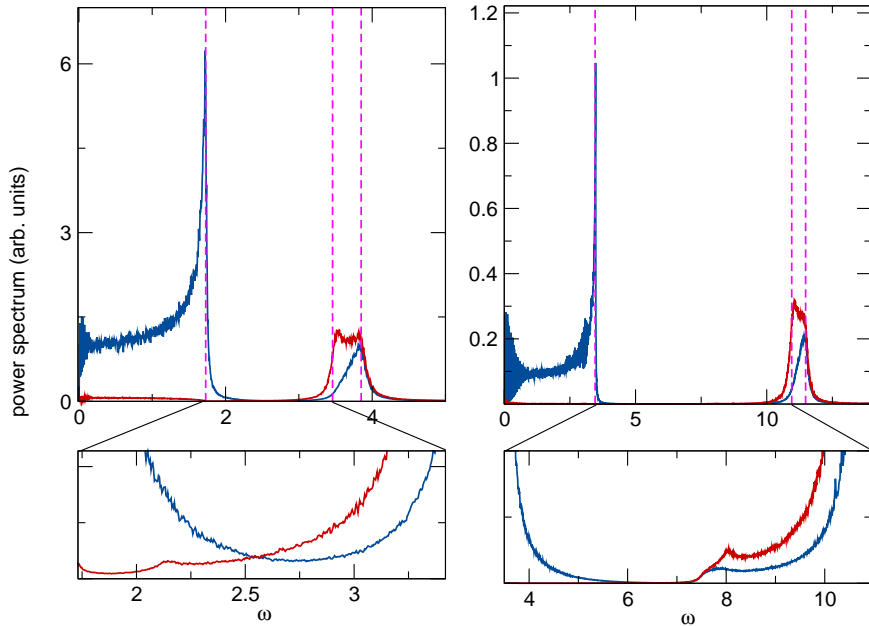


Figure 4: The spectra of momentum for light (red) and heavy (blue) particles is different,  $N = 1024$ ,  $d = 1$  energy density  $e = 8.0 \cdot 10^{-4}$ . Left panels: mass ratio  $m = 1, M = 4$ , right  $m = 0.1, M = 1$ . The vertical dotted lines are the phonon band edges. The bottom panels are enlargements of the gap regions. Notice how in the bottom-right panel the small peak at  $\omega \approx 8$  is only present in the spectrum of light masses: this can be interpreted as due to localized oscillations with almost no component on the heavy particles.

The simulations suggest that there is a separation of time scales in which the fast dynamics is driven by the slow motion of the heavy masses. One may thus argue about the consequences of such driving on transient energy localization. This will be discussed in the next section by means of a multi-scale approach.



## 5. Approximate dynamics

The first step is to distinguish fast and slow time-scales. Let us first introduce the smallness parameter  $\varepsilon = \sqrt{m/M} \ll 1$ . To lowest order, the harmonic bands are thus given by

$$\omega \approx \sqrt{2k}\varepsilon |\sin q| \quad (12)$$

$$\omega \approx \sqrt{2k} \left( 1 + \frac{\varepsilon^2}{2} \cos^2 q \right) \quad (13)$$

In this limit the acoustic band is of order  $\omega_0\varepsilon$  and the optical is in between  $\omega_0$  and  $\omega_0(1 + \varepsilon^2/2)$  where  $\omega_0 \equiv \sqrt{2k}$ . The equation of motion are

$$m\ddot{v}_n = -F(u_n - v_n) + F(v_n - u_{n-1}) \quad ; \quad (14)$$

$$m\ddot{u}_n = \varepsilon^2[-F(v_{n+1} - u_n) + F(u_n - v_n)] \quad (15)$$

that explicitly show how the separation of time scales occurring for  $\varepsilon \rightarrow 0$ . Already at this level, it is clear that the first eq. (15) is an equation for the oscillator  $v_n$  subject to an effective force changing slowly with the variables  $u_n, u_{n-1}$ . So it is in principle possible that such a force may destabilizes the oscillator, at least for a certain time interval. This can be seen for instance for  $v_n \ll u_n, u_{n-1}$ . On the rhs of the eq. (15) for  $m\ddot{v}_n$  there appears a term  $\approx (F'(u_n) + F'(-u_{n-1}))v_n$  that can lead to transient growth of the energy if  $F'(u_n) + F'(-u_{n-1}) > 0$  for a sufficiently large time lapse. A rough estimate of such time scale is given by the inverse of the acoustic band edge, that from (13) is of order  $\varepsilon^{-1}$ . Altogether, such heuristic argument suggests that a transient localization of energy can be seen on a relatively long time interval for  $\varepsilon$  small enough.

The argument can be made more precise by a multiple-scale analysis for weak non-linearity. This amounts to an expansion of the coordinates of the form

$$u_n = U_n + \varepsilon U_n^{(1)} + \varepsilon^2 U_n^{(2)} + \dots; \quad v_n = V_n + \varepsilon V_n^{(1)} + \varepsilon^2 V_n^{(2)} + \dots$$

where the  $U$  and  $V$  are a priori all functions of the time-scales  $(t, T = \varepsilon t)$ . The details of the calculation are given in the Appendix. Performing the calculation up to order  $\varepsilon^2$  and under some simplifying assumption, a closed set of equation can be obtained see eq. (31) in the Appendix.

A detailed analysis of the resulting equations will be reported elsewhere. Here we limit ourselves to some qualitative considerations. Indeed, a useful insight can be achieved by considering the following equations

$$\begin{aligned} (i - \varepsilon)\Omega_0 \frac{d\mathcal{A}_n}{dT} &= -\frac{3}{2}\beta|\mathcal{A}_n|^2\mathcal{A}_n - \alpha(U_n - U_{n-1})\mathcal{A}_n \quad (16) \\ \frac{d^2U_n}{dT^2} &= \frac{1}{2}\omega_0^2[U_{n+1} - 2U_n + U_{n-1}] \end{aligned}$$

where the complex variable  $\mathcal{A}_n$  represents the slow modulation of the amplitude of the light particle

$$v_n(t, T) = \frac{U_n + U_{n-1}}{2} + \mathcal{A}_n(T)e^{i\Omega_0 t} + \mathcal{A}_n^*(T)e^{-i\Omega_0 t} \quad (17)$$

(this last equation approximates the sum of eqs. (22) and (26) below). This model can be regarded as a crude approximation where the coupling terms in eq. (31) below and the fast component  $U_n^{(2)}$  are ignored.

Despite the underlying simplifications, the first equation in (16) is insightful: it shows that the fluctuations of the slow field appear multiplicatively and can be regarded as a dissipation or gain term depending on the sign of the local stretch  $U_n - U_{n-1}$ . At finite temperatures, such a quantity will be an incoherent superposition of all the harmonic modes of the harmonic chain in (16). Thus, it is basically a kind of slowly-varying noise with a finite bandwidth driving the light particles.

Following this idea, in Fig. 5 we report a simulation of Langevin simulation where the equation for  $\mathcal{A}_n$  is as in eq. (16) while  $U_n - U_{n-1}$  is replaced by an Ornstein-Uhlenbeck process  $z$ ,  $\dot{z} = -\varepsilon z + \xi$ . Here,  $\xi$  is a random Gaussian process with standard deviation  $\sigma$ . The random variable  $z$  has a bandwidth of size  $O(\varepsilon)$  that mimics the dynamics of  $U_n$  on the slow scale. As seen in the bottom panel of Fig. 5, the wavelet analysis reproduces qualitatively the transient localization in frequency generated by the nonlinear frequency shift. We thus conclude that our interpretation is supported by the effective model.

Finally, we may discuss the possible role of additional damping on the transient localization. If an additional small dissipation is added which is of the same order of  $\varepsilon$ , the dynamics should be qualitatively the same. Within the limitation of the simplified model (16), we may expect the local instability mechanism should be robust, albeit slightly inhibited by a larger dissipation level.

## 6. Conclusions

We have argued that transient nonlinear localization in the gap of the diatomic Lennard-Jones chain at finite temperature originates from two different mechanism. One is the thermal excitation of genuine DB. The second is an effect of coupling of the light particles with slow vibrations of the heavy ones. The quadratic term of the force generate an effective potential that can lead to transient grow of local energy on time scales the can be relatively long for small mass ratios. As a consequence, the spots of localized energy created in this way are different in nature from thermally generated breathers. Thus, some caution is needed in the interpretation of transient localization event. This is a novel issue that, in our view, should be considered in the data interpretation.

The heuristics and numerical observations are supported by a multiple-scale calculation based on the natural time-scale separation. As a further simplification, we considered an effective single-particle model that allows for some insight of the chain dynamics. We remark that multiple scale approach used here is different from the standard one employed to study DB solutions based on envelope instability of zone-boundary modes [8]. Here we rather consider the question of how the fast dynamics is affected by slow motion and should thus be regarded as a complementary approach.

## Acknowledgements

This research did not receive any specific grant from funding agencies in the public, commercial, or not-for-profit sectors. We thank Stefano Iubini for a careful reading of the manuscript.

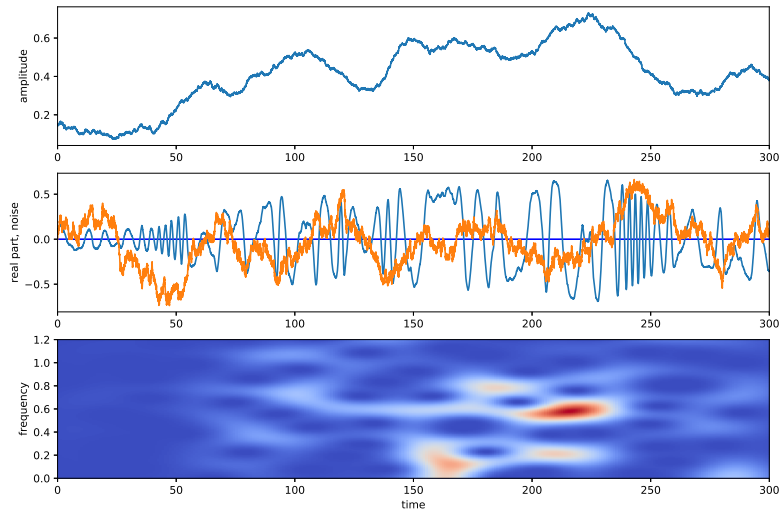


Figure 5: Langevin simulation of equation for  $\mathcal{A}_n$  as in eq. (16) where  $U_n - U_{n-1}$  is replaced by an Ornstein-Uhlenbeck process  $z$  with correlation time  $\varepsilon^{-1}$  and variance 0.1.  $\varepsilon = 0.025$ ,  $\alpha = 4\Omega_0$ ,  $\beta = 2\Omega_0/3$ . Top: oscillator amplitude  $|\mathcal{A}_n|^2$ . Middle panel: real part of  $\mathcal{A}_n$  and the process  $z$ ; Bottom: the square modulus of the Gabor transform of  $\mathcal{A}_n$  displays transient oscillations in correspondence with the instantaneous growth of the oscillator amplitude.

## Appendix

We give here some basic details of the multiple-scale expansion leading to the effective equations. Derivatives are expanded at different orders

$$O(1) : \frac{d}{dt} \frac{dV_n}{dt} \quad (18)$$

$$O(\varepsilon) : 2 \frac{d}{dt} \frac{dV_n}{dT} + \frac{d}{dt} \frac{dV_n^{(1)}}{dt} \quad (19)$$

$$O(\varepsilon^2) : \frac{d}{dT} \frac{dV_n}{dT} + 2 \frac{d}{dt} \frac{dV_n^{(1)}}{dT} + \frac{d}{dt} \frac{dV_n^{(2)}}{dt} \quad (20)$$

Similar expansions hold for the variables  $U$ . It is matter to solve the resulting equation order-by-order. We then assume an expansion of the force as  $F(0) = 0$ ,  $F'(0) = m\omega_0^2$

$$F(x) = -m\omega_0^2 x - \alpha x^2 - \beta x^3 \dots = -m\omega_0^2 x + \varepsilon F_{nl}(x)$$

As far as smallness of nonlinearity is concerned, we have here assumed that  $\alpha$  and  $\beta$  are of the same order of  $\varepsilon$  but one may as well think of  $\beta \sim \varepsilon^2$  in this case  $\beta$  does not enter up to second order. To zeroth order  $\varepsilon = 0$  the problem reduces to uncoupled linear oscillators

$$\begin{aligned} \frac{d}{dt} \frac{dV_n}{dt} &= \omega_0^2 (U_n + U_{n-1} - 2V_n) \\ \frac{d}{dt} \frac{dU_n}{dt} &= 0 \end{aligned} \quad (21)$$

We can thus take  $U_n(t, T)$  to be independent of  $t$  and solve the above as

$$V_n(t, T) = \frac{U_n + U_{n-1}}{2} + A_n(T) e^{i\Omega_0 t} + c.c. \quad (22)$$

where  $\Omega_0 = \sqrt{2}\omega_0$  the upper band edge of the optical band. The interpretation is simply that oscillations of the light particles are decoupled and occur around the center of mass of the neighboring heavy particles with a slow modulation given by the complex amplitudes  $A_n(T)$ .

To first order in  $\varepsilon$

$$\begin{aligned} 2 \frac{d}{dt} \frac{dV_n}{dT} + \frac{d}{dt} \frac{dV_n^{(1)}}{dt} &= \omega_0^2 (U_n^{(1)} + U_{n-1}^{(1)} - 2V_n^{(1)}) - F_{nl}(U_n - V_n) + F_{nl}(V_n - U_{n-1}) \\ 2 \frac{d}{dt} \frac{dU_n}{dT} + \frac{d}{dt} \frac{dU_n^{(1)}}{dt} &= 0 \end{aligned}$$

Taking into account the zeroth order, we get

$$\begin{aligned} U_n - V_n &= \frac{U_n - U_{n-1}}{2} - A_n(T) e^{i\Omega_0 t} + c.c. \\ V_n - U_{n-1} &= \frac{U_n - U_{n-1}}{2} + A_n(T) e^{i\Omega_0 t} + c.c. \end{aligned} \quad (23)$$

That can be substituted in the equations above to yield

$$\begin{aligned} \frac{d}{dt} \frac{dV_n^{(1)}}{dt} - \omega_0^2 (U_n^{(1)} + U_{n-1}^{(1)} - 2V_n^{(1)}) &= -2 \frac{d}{dt} \frac{dV_n}{dT} - F_{nl}(U_n - V_n) + F_{nl}(V_n - U_{n-1}) \\ \frac{d}{dt} \frac{dU_n^{(1)}}{dt} &= 0. \end{aligned}$$

The second equation implies  $U_n^{(1)}(T)$  so that  $V_n^{(1)}$  oscillates with frequency  $\Omega_0$  on the fast scale. To avoid secular terms, one has to impose that the right hand side in the first equation does not contain terms in  $e^{\pm i\Omega_0 t}$ , obtaining the condition

$$2i\Omega_0 \frac{dA_n}{dT} = -3\beta|A_n|^2 A_n - 2\alpha(U_n - U_{n-1})A_n \quad (24)$$

which has the familiar form of the amplitude equation for a nonlinear oscillator except for the explicit dependence on the variables  $U_n$  that, to this order are yet to be determined. Actually, the equation for  $V^{(1)}$  is nonhomogeneous

$$\frac{d}{dt} \frac{dV_n^{(1)}}{dt} - \omega_0^2 (U_n^{(1)} + U_{n-1}^{(1)} - 2V_n^{(1)}) = -2\beta A_n^3 e^{3i\Omega_0 t} + cc \quad (25)$$

which would require considering the third harmonic of the nonlinear oscillations. To keep things simpler we neglect at all the rhs of eq. (25) so that

$$V_n^{(1)}(t, T) = \frac{U_n^{(1)} + U_{n-1}^{(1)}}{2} + A_n^{(1)}(T)e^{i\Omega_0 t} + c.c. \quad (26)$$

To second order in  $\varepsilon$

$$\begin{aligned} \frac{d}{dT} \frac{dV_n}{dT} + 2 \frac{d}{dt} \frac{dV_n^{(1)}}{dT} + \frac{d}{dt} \frac{dV_n^{(2)}}{dt} &= \\ \omega_0^2 (U_n^{(2)} + U_{n-1}^{(2)} - 2V_n^{(2)}) - F'_{nl}(U_n - V_n)(U_n^{(1)} - V_n^{(1)}) + F'_{nl}(V_n - U_{n-1})(V_n^{(1)} - U_{n-1}^{(1)}) & \\ \frac{d}{dT} \frac{dU_n}{dT} + 2 \frac{d}{dt} \frac{dU_n^{(1)}}{dT} + \frac{d}{dt} \frac{dU_n^{(2)}}{dt} &= \omega_0^2 [U_{n+1} - 2U_n + V_n] \end{aligned}$$

Using previous orders, eq.(23)

$$\begin{aligned} \frac{d}{dt} \frac{dV_n^{(2)}}{dt} - \omega_0^2 (U_n^{(2)} + U_{n-1}^{(2)} - 2V_n^{(2)}) &= \\ = -\frac{d}{dT} \frac{dV_n}{dT} - 2 \frac{d}{dt} \frac{dV_n^{(1)}}{dT} - F'_{nl}(U_n - V_n)(U_n^{(1)} - V_n^{(1)}) + F'_{nl}(V_n - U_{n-1})(V_n^{(1)} - U_{n-1}^{(1)}) & \\ \frac{d}{dt} \frac{dU_n^{(2)}}{dt} = -\frac{d}{dT} \frac{dU_n}{dT} + \frac{1}{2} \omega_0^2 [U_{n+1} - 2U_n + U_{n-1}] + (A_{n+1} + A_n)e^{i\Omega_0 t} + cc & \quad (27) \end{aligned}$$

A solution of the second equation above is

$$\frac{d}{dT} \frac{dU_n}{dT} = \frac{1}{2} \omega_0^2 [U_{n+1} - 2U_n + U_{n-1}] \quad (28)$$

$$U_n^{(2)}(t, T) = -\frac{A_{n+1} + A_n}{\Omega_0^2} e^{i\Omega_0 t} + c.c. \quad (29)$$

This shows that the heavy masses have also a fast component to order  $\varepsilon^2$ . Once more, to avoid secular term we must impose that terms in  $e^{\pm i\Omega_0 t}$  in the first of eqs.(27) are identically zero yielding

$$2i\Omega_0 \frac{dA_n^{(1)}}{dT} = -\frac{d}{dT} \frac{dA_n}{dT} - 2\alpha \left[ (U_n - U_{n-1})A_n^{(1)} + (U_n^{(1)} - U_{n-1}^{(1)})A_n \right] + \omega_0^2 (U_n^{(2)} + U_{n-1}^{(2)}) \quad (30)$$

Note that the terms in  $\beta$  do not enter. To close the system we need an equation for  $U_n^{(1)}$  which however seems undetermined at least at this order (probably this would require a  $\varepsilon^3$  terms). If we suppose  $U_n^{(1)} = 0$ , using eq. (29) we have the equation for  $A_n^{(1)}$

$$2i\Omega_0 \frac{dA_n^{(1)}}{dT} = -\frac{d}{dT} \frac{dA_n}{dT} - 2\alpha(U_n - U_{n-1})A_n^{(1)} - \frac{1}{2}(A_{n+1} + 2A_n + A_{n-1}). \quad (31)$$

Finally, we can write a closed set of equations for  $U_n + \varepsilon^2 U_n^{(2)}$  and the modulation  $A_n = A_n + \varepsilon A_n^{(1)}$  summing the corresponding equations for first and second order. To obtain the dissipation term as in (16), in (31) we make the replacement

$$\frac{d}{dT} \frac{dA_n}{dT} \approx i\Omega_0 \frac{dA_n}{dT}$$

which is justified within the slowly-variable amplitude hypothesis. The simplified equations (16) are obtained neglecting  $U_n^{(2)}$  and the last term in (31).

## References

- [1] S. Lepri (Ed.), Thermal transport in low dimensions: from statistical physics to nanoscale heat transfer, Vol. 921 of Lect. Notes Phys, Springer-Verlag, Berlin Heidelberg, 2016.
- [2] G. Tsironis, S. Aubry, Slow relaxation phenomena induced by breathers in nonlinear lattices, Physical review letters 77 (26) (1996) 5225.
- [3] F. Piazza, S. Lepri, R. Livi, Slow energy relaxation and localization in 1d lattices, Journal of Physics A: Mathematical and General 34 (46) (2001) 9803.
- [4] B. Rumpf, Simple statistical explanation for the localization of energy in nonlinear lattices with two conserved quantities, Physical Review E 69 (1) (2004) 016618.
- [5] S. Iubini, R. Franzosi, R. Livi, G.-L. Oppo, A. Politi, Discrete breathers and negative-temperature states, New Journal of Physics 15 (2) (2013) 023032.
- [6] S. Iubini, L. Chirondojan, G.-L. Oppo, A. Politi, P. Politi, Dynamical freezing of relaxation to equilibrium, Physical review letters 122 (8) (2019) 084102.
- [7] S. Iubini, S. Lepri, R. Livi, G.-L. Oppo, A. Politi, A chain, a bath, a sink, and a wall, Entropy 19 (9). doi:10.3390/e19090445.  
URL <https://www.mdpi.com/1099-4300/19/9/445>
- [8] S. Flach, A. V. Gorbach, Discrete breathers—advances in theory and applications, Physics Reports 467 (1-3) (2008) 1–116.
- [9] Y. A. Kosevich, S. Lepri, Modulational instability and energy localization in anharmonic lattices at finite energy density, Physical Review B 61 (1) (2000) 299.
- [10] M. Eleftheriou, S. Flach, G. Tsironis, Breathers in one-dimensional nonlinear thermalized lattice with an energy gap, Physica D: Nonlinear Phenomena 186 (1) (2003) 20–26.
- [11] M. Ivanchenko, O. Kanakov, V. Shalfeev, S. Flach, Discrete breathers in transient processes and thermal equilibrium, Physica D: Nonlinear Phenomena 198 (1-2) (2004) 120–135.
- [12] J. Farago, The notion of persistence applied to breathers in thermal equilibrium, Physica D: Nonlinear Phenomena 237 (8) (2008) 1013 – 1020.  
doi:<http://dx.doi.org/10.1016/j.physd.2008.01.008>.  
URL <http://www.sciencedirect.com/science/article/pii/S0167278908000110>

- [13] K. Forinash, W. C. Lang, Frequency analysis of discrete breather modes using a continuous wavelet transform, *Physica D: Nonlinear Phenomena* 123 (1-4) (1998) 437–447.
- [14] M. Eleftheriou, S. Flach, Discrete breathers in thermal equilibrium: distributions and energy gaps, *Physica D: Nonlinear Phenomena* 202 (1-2) (2005) 142–154.
- [15] L. Khadeeva, S. Dmitriev, Lifetime of gap discrete breathers in diatomic crystals at thermal equilibrium, *Phys. Rev. B* 84 (2011) 144304. doi:10.1103/PhysRevB.84.144304.  
URL <http://link.aps.org/doi/10.1103/PhysRevB.84.144304>
- [16] M. Mareschal, A. Amellal, Thermal-conductivity in a one-dimensional Lennard-Jones chain by molecular-dynamics, *Phys. Rev. A* 37 (6) (1988) 2189–2196.
- [17] Lepri S., Sandri P., Politi A., The one-dimensional Lennard-Jones system: collective fluctuations and breakdown of hydrodynamics, *The European Physical Journal B - Condensed Matter and Complex Systems* 47 (4) (2005) 549–555.
- [18] R. Livi, M. Spicci, R. MacKay, Breathers on a diatomic FPU chain, *Nonlinearity* 10 (6) (1997) 1421.
- [19] P. Maniadis, A. Zolotaryuk, G. Tsironis, Existence and stability of discrete gap breathers in a diatomic Fermi-Pasta-Ulam chain, *Physical Review E* 67 (2003) 046612.
- [20] A. V. Gorbach, M. Johansson, Discrete gap breathers in a diatomic Klein-Gordon chain: Stability and mobility, *Physical Review E* 67 (6) (2003) 066608.
- [21] A. Zolotaryuk, P. Maniadis, G. Tsironis, Discrete gap breathers in chains with strong hydrogen bonding, *Physica B: Condensed Matter* 296 (1) (2001) 251–258.
- [22] G. James, M. Kastner, Bifurcations of discrete breathers in a diatomic Fermi–Pasta–Ulam chain, *Nonlinearity* 20 (3) (2007) 631.
- [23] N. Boechler, G. Theocharis, S. Job, P. Kevrekidis, M. A. Porter, C. Daraio, Discrete breathers in one-dimensional diatomic granular crystals, *Physical review letters* 104 (24) (2010) 244302.
- [24] V. Kannan, A. Dhar, J. L. Lebowitz, Nonequilibrium stationary state of a harmonic crystal with alternating masses, *Phys. Rev. E* 85 (2012) 041118. doi:10.1103/PhysRevE.85.041118.  
URL <https://link.aps.org/doi/10.1103/PhysRevE.85.041118>
- [25] T. Hatano, Heat conduction in the diatomic Toda lattice revisited, *Physical Review E* 59 (1) (1999) R1.
- [26] D. Xiong, Y. Zhang, H. Zhao, Heat transport enhanced by optical phonons in one-dimensional anharmonic lattices with alternating masses, *Phys. Rev. E* 88 (2013) 052128. doi:10.1103/PhysRevE.88.052128.  
URL <https://link.aps.org/doi/10.1103/PhysRevE.88.052128>
- [27] G. Huang, B. Hu, Asymmetric gap soliton modes in diatomic lattices with cubic and quartic nonlinearity, *Phys. Rev. B* 57 (1998) 5746–5757. doi:10.1103/PhysRevB.57.5746.  
URL <http://link.aps.org/doi/10.1103/PhysRevB.57.5746>
- [28] B. Hu, G. Huang, M. G. Velarde, Dynamics of coupled gap solitons in diatomic lattices with cubic and quartic nonlinearities, *Physical Review E* 62 (2) (2000) 2827.
- [29] A. Porubov, I. Andrianov, Nonlinear waves in diatomic crystals, *Wave Motion* 50 (7) (2013) 1153–1160.
- [30] R. I. McLachlan, P. Atela, The accuracy of symplectic integrators, *Nonlinearity* 5 (2) (1992) 541.
- [31] A. Rivière, S. Lepri, D. Colognesi, F. Piazza, Wavelet imaging of transient energy localization in nonlinear systems at thermal equilibrium, *Phys. Rev. B* 99 (2019) 024307. doi:10.1103/PhysRevB.99.024307.  
URL <https://link.aps.org/doi/10.1103/PhysRevB.99.024307>